A NUMERICAL CFD STUDY ON THE INTEGRATION AND PERFORMANCE ENHANCEMENT OF OSCILLATING AEROFOIL WIND ENERGY CONVERTERS INTO BUILDINGS

K. Calautit[1] and C. Johnstone[1],
[1]University of Strathclyde, Glasgow, Scotland

ABSTRACT

This study investigated the wind characteristics such as areas of separation, stagnation point, concentration, and wind acceleration on different roof structures with the proposed wind energy harvesting technology using the computational fluid dynamics tool in ANSYS Fluent. The six degrees of freedom solver was used to develop a model for predicting the urban wind flow over and around the oscillating aerofoil building roof structure. Moreover, the research evaluated the impact of different parameters that affect the performance of oscillating aerofoil harvesting technologies in building roof structures. These include the effects of roof shape, placement, airflow distribution, accelerated wind velocity magnitude, and wind direction, which optimizes the potential of the oscillating aerofoil integrated into the building roof structure for harvesting energy. Two different roof shapes were examined, including the flat and pitched roofs with two various placement locations of the aerofoil. The results showed that the integration of an oscillating aerofoil into the top middle the of pitched roof installed at a distance of 600 mm from the roof surface showed higher power extraction compared to the other three models examined. This results from the acceleration of wind flow over the roof surfaces and the right placement of the aerofoil into the building roof structure. Whilst poor performance was observed for the oscillating aerofoil installed at a flat roof structure with a distance of 600 mm from the roof surface. This was due to the large recirculation areas above the flat roof, which did not provide a suitable airflow condition for the energy harvester.

KEYWORDS

Computational Fluid Dynamics (CFD); Wind Energy; Building; Oscillating Aerofoil; Roof-Mounted Wind Energy Harvesting System

INTRODUCTION AND LITERATURE REVIEW

Over the past few years, building-integrated wind energy harvesting systems (BI-WEHS) have proven their potential in generating power in a range of watts to kilowatts from the wind's kinetic energy using wind turbines coupled with generators when installed on the rooftop (Kumar et al., 2017). In spite of their potential, a few concerns arise during the installation and operation, which hampers the continuous development of the technology. These concerns include the low wind speeds, high levels of turbulence due to the surface roughness near the ground or building level, and the high cost of equipment and installation on the building.

To respond to these challenges, an oscillating aerofoil integrated into the building roof structure design is proposed in this study. The proposed design is a potential solution to extracting energy from wind flow over and around buildings. This design comprises an oscillating aerofoil-based energy harvesting device integrated into the building roof structure. From a theoretical research perspective, there have been many studies (Zhu et al., 2019; Liu et al., 2016; Vagner et al., 2015; Ledo et al., 2011; Kinsey et al., 2008) on the energy harvesting performance of oscillating aerofoils by using both numerical and experimental methods. However, there is a knowledge gap in the literature concerning the potential integration of an oscillating aerofoil energy harvester onto a building structure for power extraction and configuring the roof geometry to enhance energy extraction performance.

The aim of the study is to determine the effects of airflow distribution toward an oscillating aerofoil when integrated into the building roof structure. This study will also establish an optimum placement location for an oscillating aerofoil on a flat and pitched roof building structure using the ANSYS Computational Fluid Dynamics (CFD) software. Moreover, the CFD results will identify the effect of the roof shape on the energy harvesting performance of an oscillating aerofoil. The six degrees of freedom (6 DOF) method coupled with CFD simulation will be used to calculate the rotational movement and fluid field of the oscillating aerofoil integrated into the building roof structure. This solver will predict and examine the dynamic behaviour of an oscillating aerofoil integrated into the building roof structure. Moreover, the influence of the optimal placement of the integrated design on the energy harvesting performance into the building roof structure will be evaluated in the CFD results to generate maximum wind energy. The CFD results will provide a qualitative assessment of the best places on the roof where the oscillating aerofoil will be installed. A comparative analysis was conducted for four different integrated design models to investigate the dynamic behaviour of the torque, pitch oscillation, and frequency. Also, the flat and pitched roof building structures were selected to see the acceleration effects on the building surfaces.

RESEARCH METHODOLOGY

This section provides the development of the proposed design of an oscillating aerofoil integrated into the building roof structure for an energy harvesting system. The ANSYS Design Modeler and Fluent will be used to create the CFD model and run simulations. The CFD model, Fluent set-up, and model validation will further be discussed to encourage the future advancement of computational models that can be applied to create engineering predictions.

Modeled parameters

Four different models were investigated in this study to examine the energy harvesting potential of the proposed design. These include the aerofoil that is integrated into a distance of 600 mm and 2100 mm from the top middle of the flat roof building structure, and the other design includes the aerofoil integrated into the top middle of a pitched roof building structure with a distance of 600 mm and 2100 mm from each other. The aerofoil profile is NACA 0012 with a centre of rotation that is positioned at 0.25 meters of the chord length. The dimensions of NACA 0012 are 1 meter wing span and 1 meter chord length.

CFD simulation model

Figure 1 demonstrates the dimensions of the three-dimensional CFD model of the computational domain and building roof structure created in Design Modeler. The measurements of the roof building structure were based on the validated CFD model of the building with a pitched roof building.

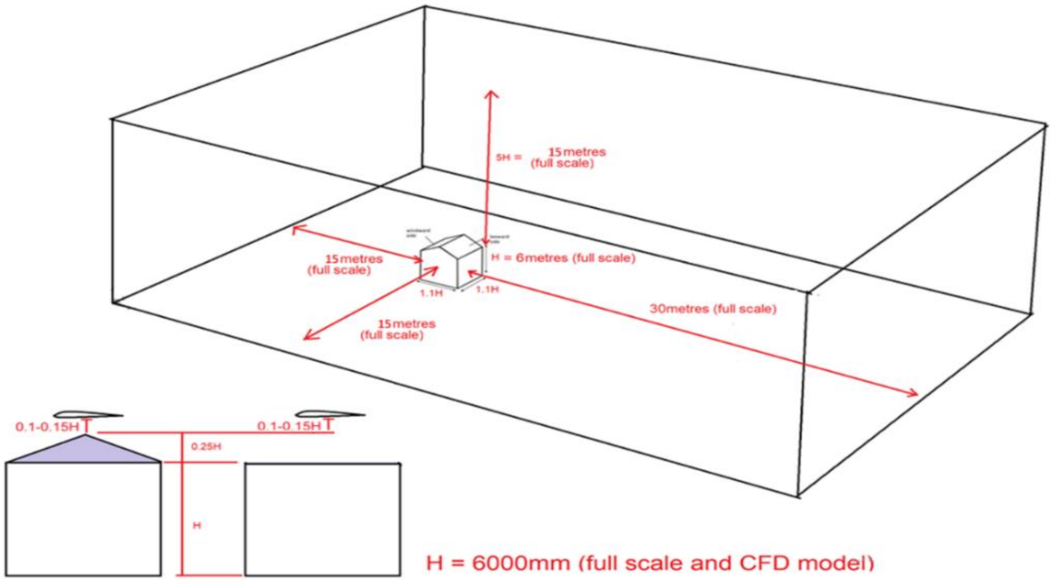

Figure 1. The dimension of the 3D computational model created in Design Modeler

CFD dynamic mesh set-up

The fluid flow will be modelled using the k-epsilon turbulence model to calculate the computational fluid dynamics simulations, as it is a well-established tool for examining the flows above and around buildings. The dynamic mesh in ANSYS Fluent software will be used to simulate the airflow around the oscillating aerofoil and building structure. The Reynolds Averaged Navier-Stokes (RANS) turbulence models with Semi-Implicit Method for Pressure-Linked Equations (SIMPLE) velocity-pressure coupling algorithm with the second-order upwind discretisation will be used in this study. The boundary conditions set in this simulation series consist of a velocity inlet with a constant speed of 3 m/s and a pressure outlet. The aerofoil surface is considered the wall. The dynamic mesh in 1 degree of freedom (DOF) will be applied in this simulation to model the vibration. The aerofoil has been set as a rigid body and fluid interior, deforming with layering for boundary conditions, smoothing, and remeshing method to generate a new grid. The centre of rotation has been selected at 0.25 m on the X-axis, and the moment of inertia, weight, and centre of gravity will be obtained from the ANSYS material properties database. To model the pitch oscillation, the spring K constant has been used in this simulation, the value of K obtained from the PVC foam (rigid, closed-cell) material, and the constant to model weight force in this simulation. A NACA 0012 aerofoil integrated into the building roof structure will be modelled within a relatively computational domain in this simulation. The rotational motion with 1 degree of freedom was specified to identify the type of motion of a rigid body.

VALIDATION

The validation will be performed by comparing the current CFD results against experimental studies on pitch oscillating aerofoil and building roof structure. A 3D CFD model of an oscillating symmetrical aerofoil (NACA 0012) has been developed and compared to the wind tunnel experiment data conducted by (Poirel at al., 2008). The method used was the dynamic mesh with the 6 DOF solver in rotational motion (pitch) in ANSYS Fluent. It was carried out separately for the frequency values of oscillating aerofoil and wind flow around the building roof structure. A 3D CFD model of an oscillating symmetrical aerofoil (NACA 0012) has been developed and compared to the wind tunnel experiment data (Poirel et al., 2008). The airflow around the pitched roof building structures was also modelled in CFD. The airflow distribution of the experimental data from the work of (Ntinas et al., 2014) was compared with the CFD model of the pitched roof building structure. Figure 3 shows the black dots for the experiment, whilst blue (pitched roof) is for the current CFD results. Table 1 shows the comparison of frequency values at two different wind velocities. According to the results, the difference between the current CFD results with experimental data from the study of (Ntinas et al., 2014) was minimal and indicated a low error in the simulation for the pitched roof building structure. A similar trend was also observed for the different wind profiles. As shown in table 1 and figure 2, the results for both the oscillating aerofoil and building roof structure showed good agreement with the experimental data.

Table 1: Comparison of the current numerical results with the experimental data collected from the study (Poirel et al., 2008).

	Velocity (m/s)	
	6	8
Paper Frequency	1.9	2.3
Simulation Frequency	1.95	2.4
Error %	2.6	4.3

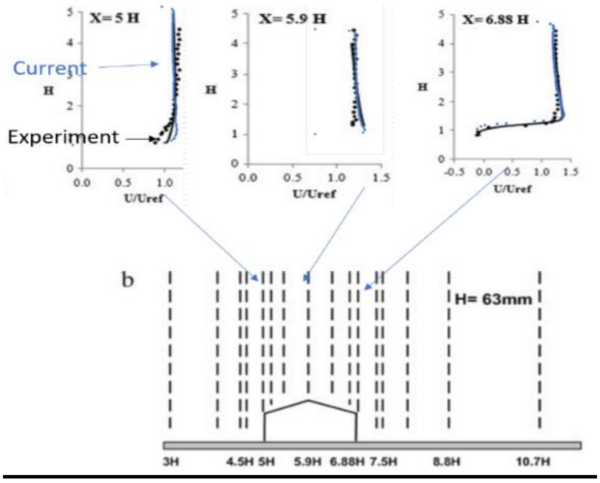

Figure 2. The comparison between numerical CFD results and experimental data (Ntinas et al., 2014)

RESULTS AND DISCUSSION

Table 2 shows the four models of an oscillating aerofoil integrated into the flat and pitched roof building structure investigated in this study. Whilst in Figures 3, 4, 5, and 6, the velocity and static pressure contours for four different models of an oscillating aerofoil integrated into flat and pitched roof building structures are demonstrated.

Table 2: The four different configurations of the integrated design of BI-WEHS

Model	Configuration	Placement	Distance
1st	Oscillating aerofoil installed at the flat roof building structure	Top middle of the rooftop	600 mm distance from the roof (near)
2nd	Oscillating aerofoil installed at the flat roof building structure	Top middle of the rooftop	2100 mm distance from the roof (far)
3rd	Oscillating aerofoil installed at the pitched roof building structure	Top middle of the rooftop	600 mm distance from the roof (near)
4th	Oscillating aerofoil installed at the pitched roof building structure	Top middle of the rooftop	2100 mm distance from the roof (far)

Air flow distribution

One of the primary requirements for determining the optimal location for installing the oscillating aerofoil is to examine the airflow characteristics, including wind velocity around the various building roof shapes, wind flow patterns, and turbulence intensity. The velocity magnitude contours for 4 different flow times, including 1 t(s) and 30 t(s) have been investigated to further evaluate airflow characteristics around and above the oscillating aerofoil integrated into the roof building structure. Figures 3 and 4 show the flow separation from the leading edge of both far and near flat roofs and large recirculation areas above the flat roof, which did not provide a suitable airflow condition for the energy harvester. Whilst in figures 5 and 6, a high streamwise velocity occurs at the top middle of the pitched roof, and large flow separation was observed over the ridge of the pitched roof. Also, the separation zone developed at the leeward side just after the roof ridge, resulting in a recirculation region. The flow separation over the roof ridge caused a reversed flow further away after the building, resulting in the recirculation behind the building.

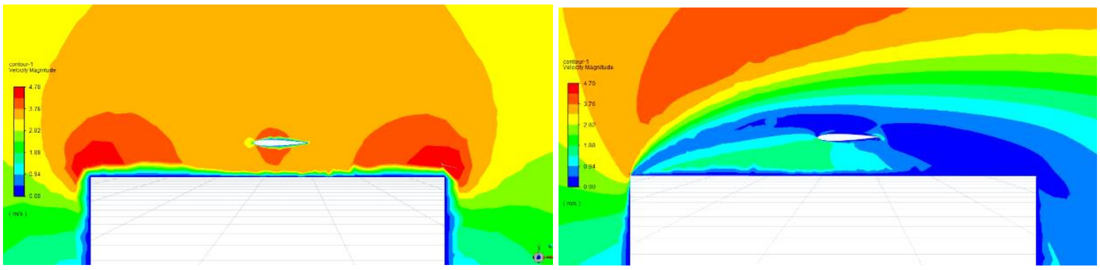

1 t(s) **30 t(s)**

Figure 3. The velocity contour of an oscillating aerofoil integrated with a distance of 600 mm into the flat roof building structure

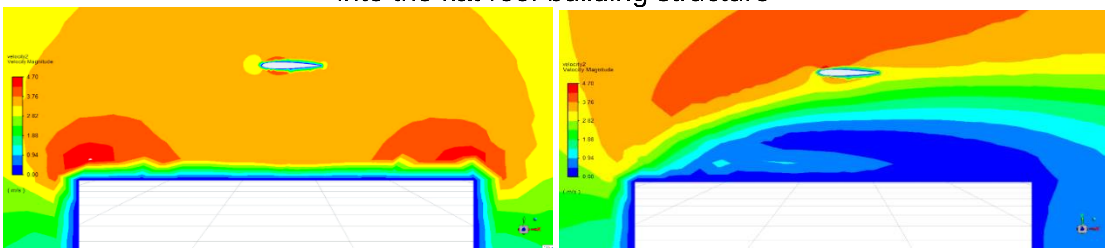

1 t(s) **30 t(s)**

Figure 4. The velocity contour of an oscillating aerofoil integrated with a distance of 2,100 mm into the flat roof building structure

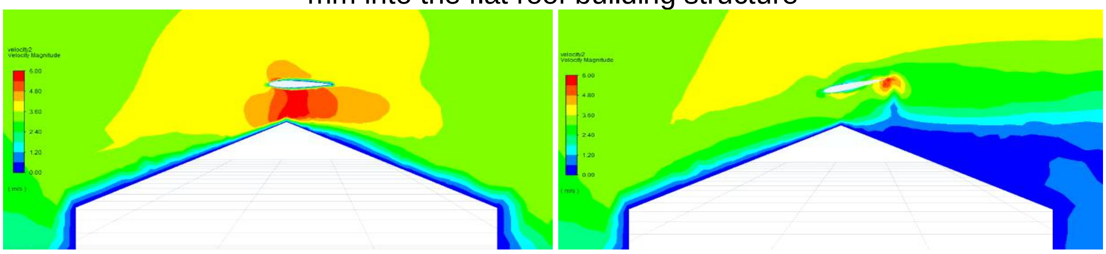

1 t(s) **30 t(s)**

Figure 5. The velocity contour of an oscillating aerofoil integrated with a distance of 600 mm into the flat roof building structure

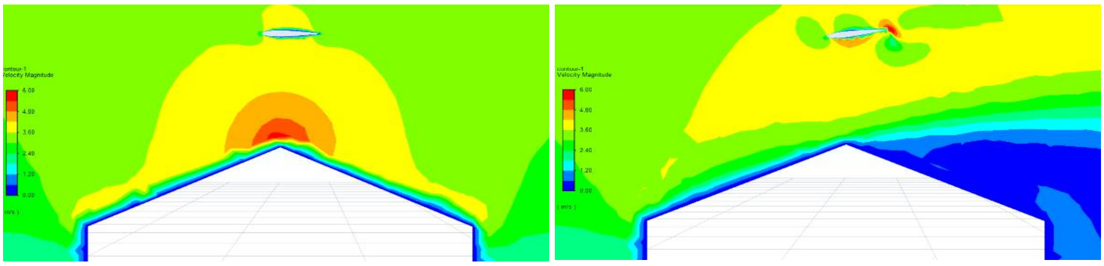

1 t(s) 30 t(s)

Figure 6. The velocity contour of an oscillating aerofoil integrated with a distance of 1200 mm into the flat roof building structure

Velocity at the leading and trailing edge of aerofoil

Different velocity magnitude points, including the leading edge and trailing edge of the aerofoil installed into the flat and pitched roof building structure, were investigated for a constant inlet wind velocity of 3 m/s. As shown in figure 7, the velocity magnitude graph provides an understanding of wind speed changes around an oscillating aerofoil surface at a constant wind velocity of 3 m/s for the 4 models. At the leading edge point of the aerofoil that is positioned at a near distance from the flat roof building structure, the velocity magnitude that started from an inlet velocity of 3 m/s showed to decrease at 0 flow time and gradually loses its oscillation until it stopped to work at 7 flow time. Whilst, a different case can be seen for the aerofoil positioned at a distance of 600 mm (near) the pitched roof building structure. The velocity magnitude also started with 3 m/s, gradually reduced to 1, increasingly achieved up to 5 m/s from 0 to 25 flow time, and oscillated at 1000 iterations. For the aerofoil installed at 2.1 m (far) of the flat roof building, the velocity magnitude increased from 4 flow time, gradually reduced at 5 flow time, and increased to 3.7 m/s up to 1000 iterations. It remained stable at 3 m/s for the model of the aerofoil installed at a 2.1 m distance from the pitched roof building structure.

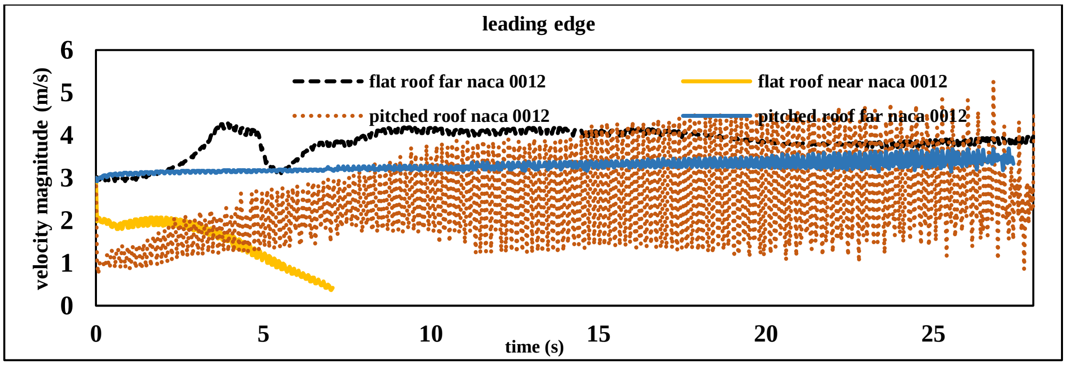

Figure 7. Velocity magnitude located at the leading edge point of the aerofoil

For the velocity magnitude located at the trailing edge point of the aerofoil, the graph in figure 8 demonstrates the 4 models, including the flat roof located near and far from the aerofoil and the pitched roof located near and far from the aerofoil. As observed from the graph, the flat roof near the aerofoil has shown similar behaviour with the velocity magnitude located at the leading edge, wherein the aerofoil oscillates and then stops at 7 flow time (s). The aerofoil installed far from the flat roof showed more stability in oscillations compared to the aerofoil installed near the flat roof building structure. The inlet velocity was set at 3 m/s and increased up to 3.7 m./s at 4 flow time but gradually decreased to 2 m/s at 5 flow time. At 6 flow time, the velocity magnitude increased from 2 m/s and remained at around 2.7 to 3 m/s in 1000 iterations. For both models of the aerofoil that is installed far and near the pitched roof building structure, the velocity magnitude showed a similar trend in oscillations, but the pitched roof naca near showed a higher wind speed until 21 flow time. Whilst the pitched roof far naca increased until it stopped to work at 27 flow time.

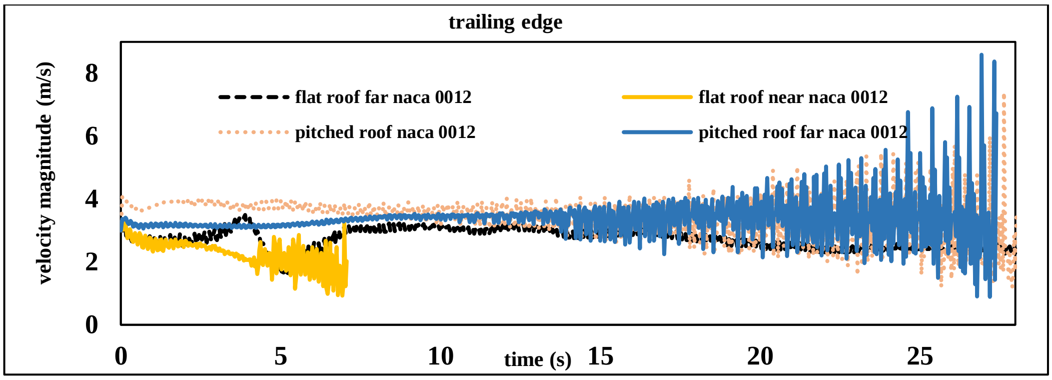

Figure 8. Velocity magnitude located at the trailing edge point of the aerofoil

DYNAMIC BEHAVIOUR OF BI-WEHS

With the objective of evaluating the energy harvesting potential of the aerofoil when integrated into the building roof structure, the torque, pitch oscillation, and frequency were calculated in 1 DOF rotation motion in ANSYS Fluent. The four models, including the aerofoil installed near and far distance from the flat roof building and the aerofoil that is installed near and far distance from the pitched roof building, were examined to optimise the energy harvesting performance of the aerofoil.

Torque

The behaviour of the torque over flow time was investigated to predict the potential for power extraction of the oscillating aerofoil under a pitch motion as power is dependent on torque force and angular velocity. Figure 9 shows the graph for the dynamic behaviour of the torque over the flow time. The CFD results demonstrate that airflow flow characteristics highly depend on the roof profiles. The oscillating aerofoil installed on the pitched roof building structure at a distance of 600 mm from the roof achieved the highest average torque value. It indicates that this mounting location and roof shape can generate more and higher power output than the other 3 models investigated in this study. This is due to the acceleration effect of the airflow over the pitched roof building structure. The lowest average torque value was obtained by the oscillating aerofoil installed on the flat roof building structure at a distance of 600 mm. This case showed that the aerofoil started oscillating and gradually became chaotic until it stopped working at 7 flow time.

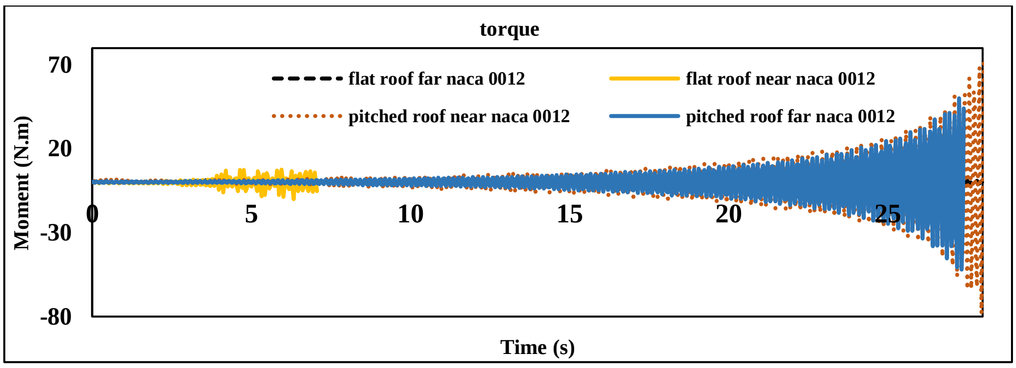

Figure 9. Torque diagram in pitch mode for a speed of 3 m / s

Pitch oscillation

In the case of pitch oscillation, the graph in figure 10 shows the dynamic behaviour of an oscillating aerofoil integrated into the building roof structure for 4 different models in 0 to 28 flow time at a constant wind speed of 3 m/s. Due to the spring constant damping application, the oscillation amplitude and natural frequency of the oscillating aerofoil were affected in all 4 models. The highest pitch oscillation was also observed for the aerofoil integrated into the pitched roof building structure. The pitch oscillation for aerofoil placed near the flat roof building structure was observed to have a higher amplitude from 0 to 7 flow time than the other 3 cases, then stopped to work after 7 flow time. The aerofoil shape and generated turbulence intensity developed by the integrated design contributed to the failure of the system. Therefore, the aerofoil integrated into the flat roof building structure is unsuitable for wind energy harvesting.

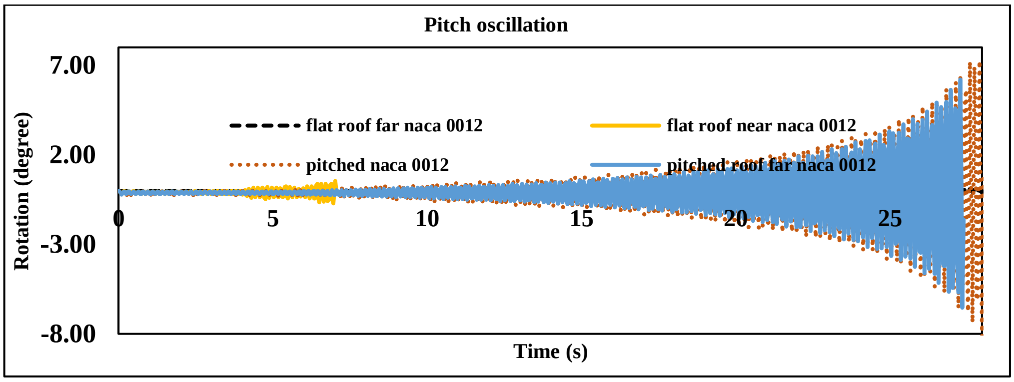

Figure 10. Pitch oscillations diagram for a speed of 3 m / s

Frequency

The frequency values were calculated from the aerofoil movement's pitch oscillations in the rotation direction per unit time. From the pitch oscillation diagram, 5 to 10 seconds were recorded for 4 cases. The highest frequency was at 6.6 Hz, whereas the lowest was at 2.8 Hz. The highest frequency value was achieved by the aerofoil installed at a pitched roof building structure with a distance of 600 mm. The lowest was obtained by the aerofoil installed on the flat roof with a distance of 600 mm. Moreover, the natural frequency of the oscillating aerofoil and amplitude of the wind wave was reduced due to the applied damping.

CONCLUSION

The CFD results clearly indicated that the power capacity of an oscillating aerofoil relies on different aspects for efficient wind energy generation. These aspects include the airflow distribution around the aerofoil and building roof structure, placement of the aerofoil into the building roof structure, dynamic behaviour of an oscillating aerofoil over time to evaluate the potential useful power, and velocity magnitude at different points, including the leading edge and trailing edge of the aerofoil. The CFD results showed the airflow distribution around the proposed design and optimum placement for the oscillating aerofoil into the building roof structure were identified to be at the top middle of the roof. The oscillating aerofoil installed at the top middle with a distance of 600 mm from the pitched roof building achieved the highest torque, which shows to have better potential power extraction for the oscillating aerofoil as compared to the other 3 models examined. Whilst a different result can be seen for the flat roof building structure. The 2 cases with an aerofoil installed into a flat roof structure indicated that it is not an ideal design for an energy harvesting system. This is mainly due to the pitched roof’s advantage of having an acceleration of wind velocity effect on the roof surfaces, which is beneficial for low wind speed areas. The modelling procedure and data generated in this work can be used to further examine the integration of the oscillating aerofoil in different building configurations and locations.

ACKNOWLEDGMENT

The authors would like to acknowledge the MAE Department at the University of Strathclyde for funding the Ph.D. research program.

<u>REFERENCES</u>

Kumar, N., Sudhakar, K., and Samykano, M., 2017. Techno- economic analysis of 1 MWp grid connected solar PV plant in Malaysia, *International Journal of Ambient Energy*.

Ledo, L., Kosasih, P., P. Cooper, P., 2011. Roof mounting site analysis for micro-wind turbines, *Renewable Energy*, 36(5), pp. 1379-1391.

Ishfaq, S. and Chaudhry, H. 2018., Numerical investigation of the optimum wind turbine sitting for domestic flat roofs, *Sustainable Buildings*, 3, pp. 14.

Zhu, B., Zhang, W., and Huang, Y., 2019. Energy extraction properties of a flapping wing with a deformable airfoil. *The Institution of Engineering and Technology Renewable Power Generation*, 13, pp. 1823-1832.

Liu, W., Xiao, Q., Zhu, Q., 2016. Passive Flexibility Effect on Oscillating Foil Energy Harvester, *American Institute of Aeronautics and Astronautics Journal*, 54, pp. 1-16.

Vagner, C., and Carlos, D., 2015. Airfoil-based piezoelectric energy harvesting by exploiting the pseudoelastic hysteresis of shape memory alloy springs, *Smart Materials and Structures*, 24.

Kinsey, T., Dumas, G., 2008. Parametric Study of an Oscillating Airfoil in Power Extraction Regime, American Institute of Aeronautics and Astronautics Journal, 46. pp.1318-1330.

Abohela, I., Hamza, N., Dudek, S., 2012. Roof Mounted Wind Turbines: The influence of roof shape, building height and urban location on wind speed.

Poirel, D., Harris, Y., Benaissa, A., 2008. Self-sustained aeroelastic oscillations of a NACA0012 airfoil at low-to-moderate Reynolds numbers, *Journal of Fluids and Structures*, 24(5), pp.700-719.

Ntinas, G. K., Zhang, G., Fragos, V. P., Bochtis, D. D., 2014. Nikita-Martzopoulou, C., Airflow patterns around obstacles with arched and pitched roofs: Wind tunnel measurements and direct simulation. *European Journal of Mechanics - B/Fluids,* 43, pp. 216-229.